THE GEOLOGICAL SOCIETY OF AMERICA®

Thermochronology constraints on Miocene exhumation in the Central Range Mountains, Trinidad

Scott Giorgis[1,†], John Weber[2,†], Sean Sanguinito[1], Carl Beno[1], and James Metcalf[3,†]

[1]*Department of Geological Sciences, State University of New York–Geneseo, 1 College Circle, Geneseo, New York 14454, USA*

[2]*Department of Geology, Grand Valley State University, Padnos Hall of Science #118, One Campus Drive, Allendale, Michigan 49401, USA*

[3]*Department of Geological Sciences, University of Colorado–Boulder, 2200 Colorado Avenue, UCB 399, Boulder, Colorado 80309, USA*

ABSTRACT

The Central Range fault zone is a continental transform that accommodates most of the present-day slip between the Caribbean and South American plates in Trinidad. Global positioning system data and paleoseismic work suggest that this zone is active today and has been active for at least the past several thousand years. The modern fault zone overprints a middle Miocene fold-and-thrust belt; therefore, the strain recorded in the Central Range fault zone is the sum of both middle Miocene and more recent events. Thermochronology data from Eocene and Oligocene sandstones in the Central Range were collected to evaluate the timing of exhumation driven by crustal shortening and thickening. (U-Th)/He zircon analysis of subhedral zircons collected from eight samples indicated that the burial temperatures of these sedimentary rocks did not exceed ~180 °C, suggesting that these grains record detrital (U-Th)/He dates. Apatite fission-track (AFT) analysis of 10 samples yielded mixed results, with cooling ages ranging from 30 to 15 Ma; however, most sites failed the χ^2 test, suggesting that multiple age cohorts are present. Pooled AFT ages suggest that rocks presently at the surface were exhumed through their AFT closure temperature ca. 11–18 Ma. Cooling and exhumation thus most likely resulted from middle Miocene shortening across the fold-and-thrust belt in response to early oblique convergence between the Caribbean and South America plates. Post-Miocene deformation associated with more recent transform tectonics has therefore resulted in more limited (<~4 km), if any, exhumation.

†giorgis@geneseo.edu; weberj@gvsu.edu; james.metcalf@colorado.edu.

INTRODUCTION

The Central Range fault zone is the active trace of the Caribbean–South American plate boundary in Trinidad, which lies just off the coast of mainland South America and Venezuela (Fig. 1; Weber et al., 2011). This fault zone overprints a long-lived, polyphase tectonic boundary that records late Mesozoic rifting, Miocene oblique convergence (Pindell et al., 1998), and, more recently, strike-slip tectonics with well-document releasing bends and possible restraining segments (Saleh et al., 2004; Weber et al., 2011). Due to reactivation, it is difficult to completely untangle the deformation, geology, and landscape elements that are due to ancient versus more recent tectonism in this zone (e.g., Giorgis et al., 2011). Understanding the neotectonics in Trinidad is critically important from a seismic risk perspective. Historic and instrumental seismic records indicate that moderately sized earthquakes are common throughout the region, but not on the Central Range fault zone (Russo et al., 1992). This observation, taken together with global positioning system (GPS) data (Fig. 2; Weber et al., 2001a, 2011; Pérez et al., 2001; Saleh et al., 2004; Churches et al., 2014) and paleoseismic trenching (Prentice et al., 2010), suggests that the Central Range fault is at least partially elastically locked and likely poses some seismic risk.

The Central Range Mountains could in principle have formed due to middle Miocene oblique convergence and/or a component of contraction within the modern primarily strike-slip system, either of which could have led to the exhumation of Cretaceous–Paleogene sedimentary rocks in the core of this range (e.g., de Verteuil et al., 2006; Fig. 1). In this study, we use new apatite fission-track (AFT) and (U-Th)/He zircon thermochronology data from the Central Range uplift to investigate the timing and infer the origin of exhumation. These data indicate that postdepositional burial of the sedimentary rocks currently exposed in the Central Range did not exceed ~180 °C (~7 km depth assuming a 25 °C/km geotherm). Subsequent oblique convergence in the middle Miocene resulted in their exhumation through the AFT closure temperature (~120 °C or 5 km depth).

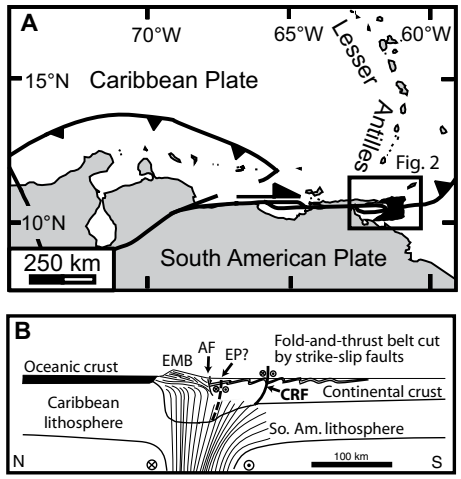

Figure 1. (A) Regional location map. Trinidad along the Caribbean–South American plate boundary where it transitions from a dextral strike-slip system into the Lesser Antilles subduction zone. (B) Schematic north-south–oriented lithospheric-scale cross section across the plate boundary through Trinidad (from Prentice et al., 2010; Teyssier et al., 2002). EMB—exhumed metamorphic belt; AF—Arima fault; EP—El Pilar fault; CRF—Central Range fault.

GEOLOGIC SETTING

Trinidad is located just offshore from Venezuela and spans the South American–Caribbean plate boundary (Fig. 1). Through most of the

GSA Bulletin; January/February 2017; v. 129; no. 1/2; p. 171–178; doi: 10.1130/B31363.1; 7 figures; 2 tables; published online 12 August 2016.

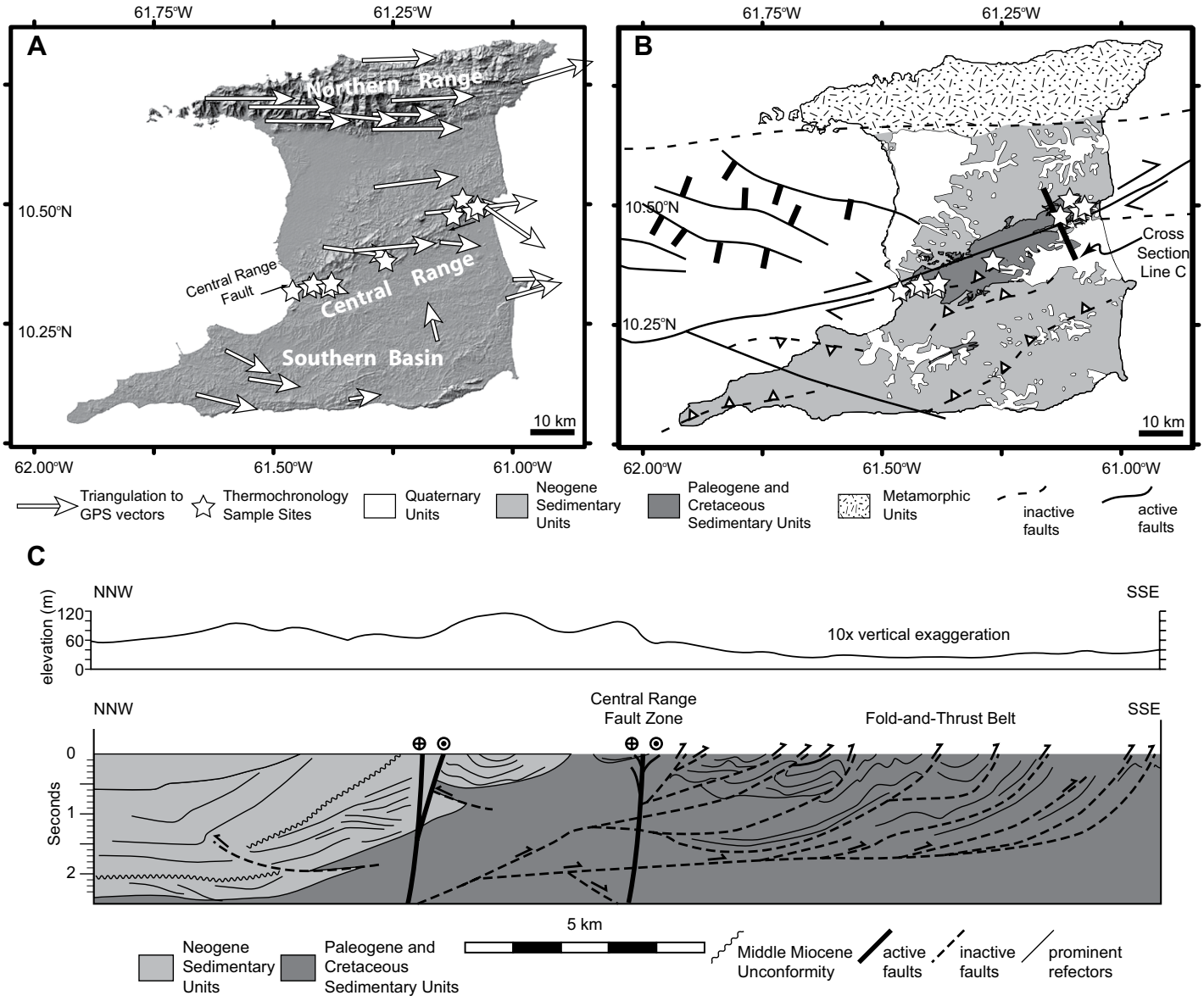

Figure 2. Location map of thermochronology sampling sites. (A) Digital elevation model and global positioning system (GPS) velocity field of Trinidad from Weber et al. (2011). Shaded relief map was generated using the Seamless Shuttle Radar data (available from U.S. Geological Survey, EROS Data Center, Sioux Falls, South Dakota). (B) Simplified geologic map of Trinidad. (C) Cross section and topographic profile through the Central Range fault zone and the middle Miocene fold-and-thrust belt modified from Pindell and Lorcan (2007). Note the vertical axis is in seconds, i.e., two-way traveltime. The Nariva Formation, which spans the Paleogene-Neogene boundary, is included with the Paleogene sediments. The geometry of the strike-slip faults is schematic. Pindell and Lorcan (2007) noted that the seismic data provide little constraint on either the dip of the vertical strike-slip faults or their geometric relationship to the thrust faults that they appear to cut. The geometry of the middle Miocene unconformity is taken from Kugler (1960). Geologic map and fault locations are modified from Flinch et al. (2000), Soto et al. (2007), and de Verteuil et al. (2006).

Cenozoic, this plate boundary initially accommodated oblique convergence in western South America, which then progressed eastward into Trinidad (e.g., Speed 1985; Pindell et al., 1998). In central Trinidad, Late Cretaceous to early Neogene rocks record passive-margin deposition prior to convergence (e.g., Erlich et al., 1993). Oblique convergence uplifted and deformed this passive-margin sequence into a fold-and-thrust belt and created the metamorphic hinterland currently exposed in the Northern Range in Trinidad (Weber et al., 2001a). Exhumation of this metamorphic core began 15–22 Ma and continued to at least the Pliocene (Cruz et al., 2007; Denison et al., 2008). South of the Northern Range, rocks of the Late Cretaceous–early Neogene passive-margin sequence are overlain by a tilted package of Pliocene–Pleistocene sedimentary rocks that consists primarily of deltaic deposits of the paleo–Orinoco River system. The boundary between these two packages of rocks is a sharply defined, middle Miocene angular unconformity (Fig. 2). The lower rocks record shortening in response to middle Mio-

cene contraction, with those above having been deposited after the cessation of contraction (e.g., Babb and Mann, 2000; Soto et al., 2011). Strain analysis of fold shape and orientation indicates that the macrofolds exposed in central Trinidad (Fig. 1C) are associated with middle Miocene shortening, rather than more recent transpressional activity (Giorgis et al., 2011).

Oblique convergence transitioned to strike-slip motion between the middle Miocene and the present, resulting in steeply dipping strike-slip faults that cut and overprint the older fold-and-thrust belt (Fig. 2C). Locally, this strike-slip motion is expressed as transtension in the Gulf of Paria pull-apart basin, and possibly transpression in the Central Range of Trinidad (Pindell et al., 1998; Babb and Mann, 2000; Weber et al., 2001b). The Caribbean plate presently moves ~20 mm/yr east relative to a fixed South America (Pérez et al., 2001; Weber et al., 2001b). Most of this motion is accommodated on the El Pilar fault in Venezuela (Pérez et al., 2001), while the plate boundary steps south onto the Central Range fault in Trinidad (Saleh et al., 2004; Weber et al., 2011). Approximately 12–15 mm/yr of the total 20 mm/yr of Caribbean–South American relative plate motion is accommodated on the Central Range fault (Weber et al., 2011). The early triangulation-to-GPS findings of Weber et al. (2011) hinted at slight obliquity of motion across the Central Range fault and the possibility that active transpression might be occurring there. More recent, higher-precision GPS-to-GPS data may suggest more limited contraction (Churches et al., 2014). Regardless, the low-relief mountains suggest that the total amount of contraction across the Central Range fault zone must be small (<3 km; Giorgis et al., 2009). Overall, the Central Range is characterized geologically as an anticlinal flower structure that exposes strongly deformed Late Cretaceous and Oligocene to Miocene sedimentary rocks in its core and mildly tilted Pliocene–Pleistocene strata on its flanks (Fig. 2; Babb and Mann, 2000; de Verteuil et al., 2006).

The Central Range clearly experienced middle Miocene contraction (e.g., Pindell et al., 1998; Babb and Mann, 2000; Soto et al., 2011), and the presence and spatial pattern of the early to middle Miocene shallow-water Tamana Limestone in the Central Range indicate limited emergence of the fold-and-thrust belt on paleotopographic highs (Erlich et al., 1993). GPS data indicate that the Central Range fault zone is currently active (e.g., Weber et al., 2011). The sharp geomorphic expression of the Central Range fault, low-relief mountains (<300 m), observations from paleoseismic trenching, and offsets imaged in offshore three-dimensional (3-D) seismic data all suggest that strike-slip faulting was also likely active earlier in the Holocene (Soto et al., 2007; Giorgis et al., 2009; Prentice et al., 2010; Weber et al., 2011). While much of the strain observed in the Central Range is due to middle Miocene contraction, it is uncertain exactly how much of the finite strain to assign to that contraction event. The folding, faulting, and topography presently observed in the Central Range could in principle be the result of deformation anytime between the middle Miocene and the modern era.

STRATIGRAPHY

Samples selected for thermochronological analysis were collected from the Chaudiere, Pointe-a-Pierre, and Nariva Formations, all of which are exposed in the exhumed core of the Central Range mountains (Fig. 3; de Vertile et al., 2006). All three formations were initially deposited along a passive margin as part of the paleo–Oronoco River fan (?) system (Vincent and Wach, 2007; Xie et al., 2010; Xie and Mann, 2014). The Chaudiere Formation is Paleocene in age (65–55 Ma) and varies up section from shale with a few beds of fine-grained sandstone into thicker, coarser sandstones and conglomerates (Kugler, 2001). The sandstone member of the Pointe-a-Pierre Formation is a sand-rich (turbiditic) "marker" unit that can be traced from east to west across the Central Range (Kugler, 2001). The age of the Pointe-a-Pierre Formation is likely early to middle Eocene (49–34 Ma) based on the diverse fossil assemblage present in the overlying Navet Formation (Vincent and Wach, 2007; Bolli, 1957). Last, the Nariva Formation consists of interbedded sandstone, siltstone, and claystone beds with occasional discontinuous coarser-grained deposits (Kugler, 2001). Biostratigraphically, the Nariva Formation spans the *Globorotalia opima opima* to the *Catapsydrax strainforthi* and *Globigerinatella insueta* zones, suggesting a depositional age in the early Miocene (24–16 Ma; Kugler, 2001).

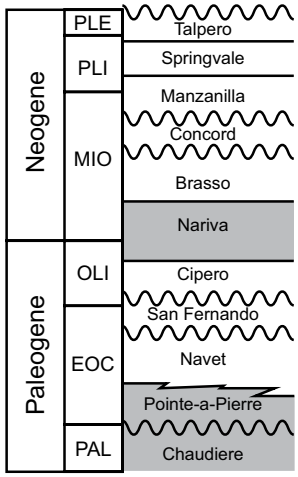

Figure 3. Stratigraphic column of Paleogene–Neogene units exposed in the Central Range, modified from Saunders (1998). Sandstone beds in the units highlighted in gray were sampled in this study. Abbreviations: PLE—Pleistocene, PLI—Pliocene, MIO—Miocene, OLI—Oligocene, EOC—Eocene, PAL—Paleocene.

APATITE FISSION TRACK

Ten AFT samples from the Chaudiere, Pointe-a-Pierre, and Nariva Formations were collected to evaluate the low-temperature exhumation history of the Central Range. In general, fission tracks in apatite are thought to totally anneal at temperatures above ~110 °C and partially anneal between 60 °C and 110 °C (e.g., Gleadow et al., 1986; Green et al., 1989). Depending on the geothermal gradient, AFT dates therefore typically reflect exhumation through the upper 2–5 km of the crust.

Methodology

The AFT data presented here were generated by Paul O'Sullivan at Apatite to Zircon, Inc. The minerals analyzed were separated using standard heavy liquid, centrifuge, and magnetic techniques. Spontaneous fission tracks in apatite were etched in 5.5 *M* HNO_3 at 21 °C for 20 s, and the samples were then subjected to ^{252}Cf irradiation to enhance confined horizontal track length detection (Donelick and Miller, 1991; Ketcham et al., 1999). Following track counting at Apatite to Zircon, Inc. (Parra et al., 2012; Donelick et al., 2005), grains were analyzed for chemistry using a laser-ablation–inductively coupled plasma–mass spectrometer (LA-ICP-MS).

Results

The χ^2 test is a statistical measure of the probability that a population of values is drawn from a single age population with a normal distribution (e.g., Galbraith, 2005). If all of the single-grain AFT ages collected from one sample were acquired during the same thermal event, then that population of single-grain ages should pass the χ^2 test. Seven of 10 AFT samples from the Central Range failed the χ^2 test (Table 1), suggesting that the single-grain ages in the population record more than one thermal event. We used two different approaches to filter the AFT age data to search for evidence of the most recent thermal event: the D_{par} kinetic parameter (Donelick et al., 2005) and the minimum age

TABLE 1. SUMMARY OF APATITE FISSION-TRACK DATA

N	Dpar (mm)	Dper (mm)	*Ns* (tracks)	Analyzed (cm^2)	S(PW) (cm^2)	±1σ S(PW) (cm^2)	x_{MS}	±1σ x_{MS}	^{43}Ca bkg:sig (dmnls)	^{236}U bkg:sig (dmnls)	χ^2	Pooled age ±1σ (Ma)
TT07-1, 10.32391°N, 61.46168°W, Pointe-a-Pierre Formation												
9	1.51	0.3	31	1.10E-04	1.74E-05	9.26E-07	15.9863	0.4851	1.95E-02	2.07E-03	0.9856	14.2 ± 2.7
TT07-3, 10.33116°N, 61.42680°W, Pointe-a-Pierre Formation												
7	1.57	0.29	69	7.57E-05	2.57E-05	9.45E-07	16.2773	0.4808	1.72E-02	2.01E-02	0.0000	21.8 ± 2.8
TT07-17, 10.33151°N, 61.38742°W, Pointe-a-Pierre Formation												
18	1.53	0.34	46	3.85E-04	2.54E-05	9.39E-07	16.2051	0.4818	2.00E-02	6.58E-01	0.0000	14.6 ± 2.3
TT07-18, 10.38267°N, 61.26959°W, Navet Formation												
23	1.57	0.34	269	2.89E-04	7.43E-05	1.84E-06	16.1180	0.4831	2.43E-02	6.34E-01	0.0000	29.1 ± 2.1
TT07-19, 10.48742°N, 61.08540°W, Pointe-a-Pierre Formation												
4	2.03	0.62	6	4.80E-05	1.45E-06	7.90E-08	15.9226	0.4860	1.88E-02	2.29E-02	0.3053	32.8 ± 13.5
TT07-20, 10.49537°N, 61.07611°W, Chaudiere Formation												
28	1.99	0.6	69	3.58E-04	2.32E-05	5.47E-07	15.8674	0.4869	2.64E-02	9.83E-02	0.0095	23.5 ± 3.0
TT08-1, 10.33774°N, 61.41866°W, Pointe-a-Pierre Formation												
12	1.4	0.28	93	1.37E-04	3.87E-05	3.58E-07	15.5373	0.3117	9.01E-02	6.34E-01	0.0000	18.6 ± 2.0
TT08-2, 10.33811°N, 61.38336°W, Pointe-a-Pierre Formation												
24	1.39	0.28	90	1.99E-04	3.92E-05	1.97E-07	15.5327	0.3137	7.62E-02	2.47E-01	0.0000	17.8 ± 1.9
TT08-3, 10.47615°N, 61.12534°W, Pointe-a-Pierre Formation												
37	1.49	0.3	291	5.07E-04	1.27E-04	7.66E-07	15.5258	0.3167	9.84E-02	2.70E-01	0.0013	17.8 ± 1.1
TT08-4, 10.51222°N, 61.10769°W, Chaudiere Formation												
4	1.48	0.2	32	4.47E-05	1.25E-05	1.93E-07	15.5211	0.3188	5.47E-02	1.02E-01	0.7528	19.9 ± 3.5

Note: N—number of grains analyzed; Dpar—diameter of etch pit parallel to crystallographic *c* axis; Dper—diameter of etch pit perpendicular to crystallographic *c* axis; *Ns*—number of spontaneous tracks measured; S(PW)—sum of $^{238}Y/^{43}Ca$ (P) and counting area (W); x_{MS}—calibration factor based on laser ablation–inductively coupled plasma–mass spectrometry of fission-track standards; bkg:sig—background to signal ratio, which is a dimensionless (dmnls) quantity; χ^2—chi-squared test results.

model (Galbraith, 2005). One possible reason for mixed grain-age populations to arise in AFT data relates to variation in annealing properties of apatite crystals (e.g., Donelick et al., 2005). While AFTs in general fully anneal by ~110 °C, annealing experiments demonstrate that some apatite crystals are much more resistant to annealing than others and do not completely anneal until reaching ~160 °C (e.g., Ketcham et al., 1999). This range in resistance to annealing is a function of apatite chemistry, track orientation, and confining pressure (e.g., Donelick et al., 2005). D_{par}, a measure of the diameter of the etch figure of an individual fission track, is a proxy measure of the annealing kinetics of apatite (Donelick, 1993). Apatites that exhibit high D_{par} values (>1.75 μm) anneal at higher temperatures, while those with lower D_{par} values (<1.75 μm) are more common and tend to anneal at lower temperatures (Carlson et al., 1999; Donelick et al., 2005). A population of apatite grains with a wide range of D_{par} values might fail the χ^2 test because a heating event could fully anneal some apatites and partially anneal others, while other crystals could even retain their detrital ages. By examining a narrower range of D_{par} values, it may be possible to isolate the signal from a single thermal event in a population that fails the χ^2 test as a whole.

For those samples that failed the χ^2 test, we used the HeFTy software package (Ketcham et al., 2000; Ketcham, 2005) to search for the largest subset of single-grain ages that passed the χ^2 test. This approach yielded age dates that passed the χ^2 test for 8 of our 10 sites (TT07-3 and TT07-18 failed). Of the eight sites that did pass, seven were consistent with a Miocene cooling event and showed no statistically significant variation with respect to position from the Central Range fault zone (Fig. 4). This group yielded a pooled age of 15.6 ± 2.6 Ma (2σ; Fig. 5). One sample from the Nariva Formation (TT07-18; 41 ± 7.8 Ma) that is interpreted to be an outlier was excluded from the mean calculation.

The minimum age model (Galbraith, 2005) is an alternate way to search for the youngest age cohort in a population of mixed ages. We used the RadialPlotter software (Vermeesch, 2009) to search for the minimum age cohort in our samples. Again, there was no statistically significant variation in minimum age as a function of position from the Central Range fault zone (Fig. 4). Sample TT07-19 could not be analyzed using this method because the uncertainty on the individual single-grain ages was too great. Excluding this sample, 9 of 10 samples yielded a pooled mean age of 13.3 ± 2.2 Ma (2σ; Fig. 5). The D_{par} and minimum age analyses of the AFT data together suggest that the rocks in the exhumed core of the Central Range cooled through ~110 °C between 18 and 11 Ma.

(U-Th)/He ZIRCON

Methodology

Zircons were concentrated using standard heavy liquid and magnetic separation techniques at State University of New York (SUNY), Geneseo, New York. Individual zircon grains were prepared for analysis at the Colorado TRaIL (Thermochronology Research and Instrumentation Laboratory) facility at the University of Colorado. Grains were first selected and characterized using a binocular microscope and then loaded into individual Nb packets. The samples were then placed in the ultrahigh-vacuum He analysis line, and He concentrations were measured with a quadrupole mass spectrometer. Degassed grains were then removed from the vacuum line, spiked with a tracer, and dissolved using standard HF and HCl acid-vapor dissolution methods in Parr dissolution vessels. U and Th concentrations were then measured on an ICP-MS at the University of California, Santa Cruz.

Results

In almost all cases, the (U-Th)/He zircon ages were older than the ages of deposition, indicating a detrital origin (Fig. 6). There were two exceptions: grains TT07-1c and TT08-1b (Table 2), which came from two different outcrops of the Pointe-a-Pierre Formation. Individually, these grains had good analytical uncertainties, which might suggest that these portions of the Pointe-a-Pierre Formation were heated to above the (U-Th)/He closure temperature of 180 °C. In both cases, however, additional zircon grains from the same samples yielded much older ages that were clearly detrital (Table 2). Possible explanations of these data include the following.

(1) In zircon, higher U concentrations yield lower closure temperatures as radiation damage creates fast pathways for He to diffuse out of the crystal (e.g., Guenthner et al., 2013). TT08-3b had an effective uranium concentration that was three to four times higher than that of the other three crystals analyzed from the same hand sample. Therefore, it is possible that TT08-3b has a lower closure temperature than the other grain from this sample and that it was reset during burial. This reasoning, however, does not hold for the other apparently postdepositional (U-Th)/He age. TT07-1c had a lower effective uranium concentration than another zircon (TT07-1b) measured from that same sample (146 vs. 188 ppm; Table 2).

(2) The age of the Pointe-a-Pierre Formation could be younger than that suggested by Vincent and Wach (2007). Based on ca. 34 Ma zircon

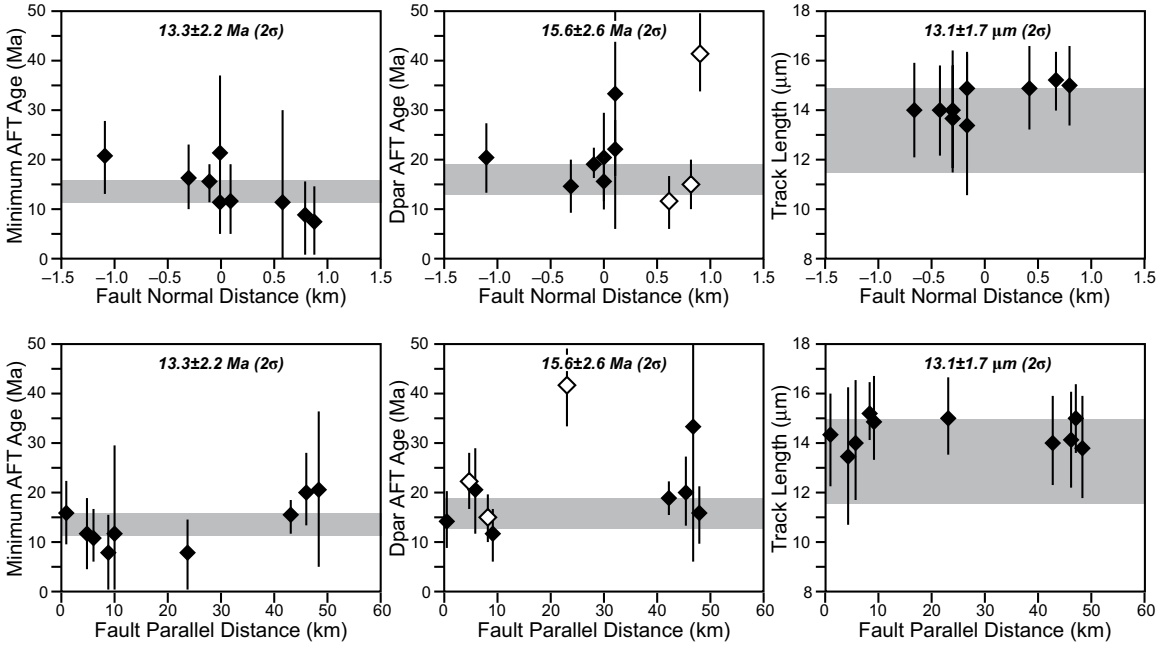

Figure 4. Apatite fission-track (AFT) and (U-Th)/He zircon ages vs. stratigraphic age. Gray bands denote the stratigraphic age range for the deposition of that formation. Note that the *x* axis is logarithmic. Dpar—a measure of the diameter of the etch figure of an individual fission track and a proxy measure of the annealing kinetics of apatite.

fission-track ages that they interpreted to be detrital, Algar et al. (1998) concluded that this formation is Oligocene in age. This interpretation allows the 31 Ma age from TT08-3b to be detrital; however, it does not explain the 19 Ma age from TT07-1c.

(3) There could have been cross contamination between samples. If a zircon from the Nariva sample contaminated TT08-3b during mineral separation, then this age would be syndepositional. Alternatively, the zircons are euhedral and show no evidence of rounding, suggesting they could be volcanic in origin. Given the proximity of the Lesser Antilles and older accreted volcanic arcs (Fig. 1), a volcanic origin for these grains is a real possibility. Again, however, cross contamination does not provide an explanation for the 19 Ma age in TT07-1c.

While it is unclear why at least one of these two zircon grains yielded anomalously young ages, the majority of the zircon (U-Th)/He data are consistent with the hypothesis that the rocks presently exposed in the core of the Central Range uplift have not experienced temperatures in excess of ~180 °C since deposition.

DISCUSSION

Previously published low-temperature thermochronology work in Trinidad has focused mostly on the Northern Range and its equivalent to the west in the Paria Peninsula in Venezuela (Algar et al., 1998; Weber et al., 2001b; Cruz et al., 2007; Denison et al., 2008). The Paria Peninsula and the Northern Range consist of hinterland metamorphic rocks with Neogene metamorphic ages and Mesozoic protolith ages (Weber et al., 2001a; Cruz et al., 2007; de Verteuil et al., 2006). Earlier Northern Range thermochronology studies presented both AFT and zircon fission-track data (ZFT). The closure temperature for ZFTs is much higher than apatite (Tagami and O'Sullivan, 2005). AFT and ZFT ages in the Paria Peninsula and in the Northern Range show that the metamorphic hinterland was exhumed rapidly at ca. 22–15 Ma in eastern Trinidad, with the ages of exhumation progressively decreasing to ca.

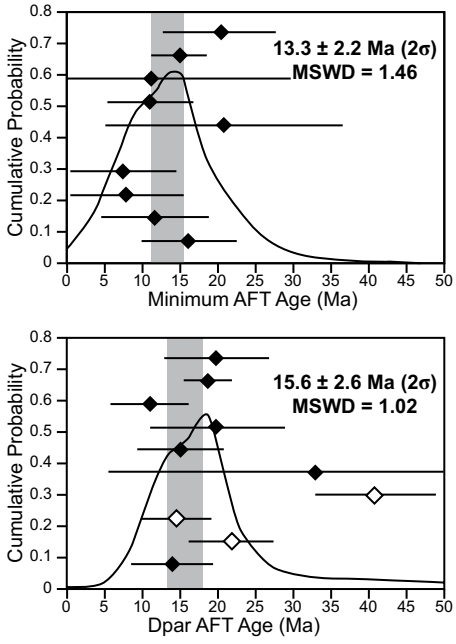

Figure 5. Apatite fission-track (AFT) age and length plotted against location in the Central Range fault zone. Note that there is no systematic variation in age or length with respect to position within the fault zone. Minimum ages were calculated using RadialPlotter by Vermeesch (2009). D_{par} ages were calculated using HeFTy (Ketcham et al., 2000; Ketcham, 2005) to sort the single-grain ages using the D_{par} kinetic parameter and find the largest populations of single grains that passed the χ^2 test. Gray bars indicate the 2σ uncertainty range about the mean. Hollow diamonds mark samples that did not pass the χ^2 test. Dpar—a measure of the diameter of the etch figure of an individual fission track and a proxy measure of the annealing kinetics of apatite; MSWD—mean square of weighted deviates.

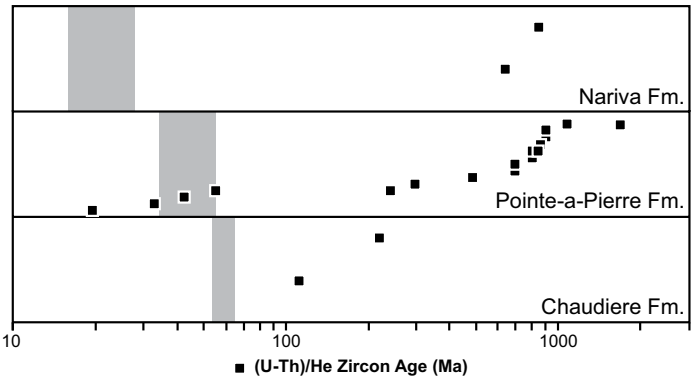

Figure 6. (U-Th)/He Zircon age data subdivided by formation. Grey zones mark age of deposition for each formation. Note the log scale on the x-axis.

4 Ma in western Trinidad and Venezuela (Cruz et al., 2007; Denison et al., 2008). AFT age data in the Northern Range vary from ca. 15 Ma in eastern Trinidad to ca. 4 Ma in the west (Denison et al., 2008). These data suggest that exhumation of the Northern Range may have been diachronous, with the early stages of exhumation driven by middle Miocene convergence and the later stages by isostatic rebound during erosion (Cruz et al., 2007; Denison et al., 2008). Regardless, the early stages of exhumation in the Northern Range are within uncertainty of the younger AFT age data from the Central Range (11–18 Ma). This similarity supports the inference that exhumation in the Northern Range and Central Range was contemporaneous and was likely driven by the same tectonic event, i.e., the oblique convergence of the Caribbean plate with South America (Fig. 6; Pindell et al., 1998; Babb and Mann, 2000; Christeson et al., 2008). The longer-lived nature of Northern Range exhumation, however, must have been driven by an additional force, possibly continued isostatic adjustment of the thicker continental crust there. We note that Babb and Mann (2000) reached a similar, but subtly different conclusion, using sedimentation patterns observed in the subsurface: 10 Ma uplift and erosion in the Northern Range, followed by subsequent uplift and erosion in the Central Range.

It is well established that the relative plate motion of Caribbean–South American was characterized by oblique convergence in the middle Miocene (e.g., Pindell et al., 1998; Babb and Mann, 2000; Soto et al., 2011) and that the Holocene system is dominated by dextral transform motion (Fig. 7; Pérez et al., 2001; Weber et al., 2001a). The thermochronological data presented here limit the amount of exhumation due to any convergent component in the modern system. Limited shortening in the modern system is supported by the low topography (Fig. 2C; Giorgis et al., 2009) and the latest, high-precision GPS-to-GPS results, which are more fault-parallel (Churches et al., 2014). If there is some small component of convergence in the active strike-slip system, the timing of initiation of the Central Range fault zone might be resolvable using lower-temperature thermochronometers such as (U-Th)/He apatite; however, our samples did not yield any apatite of appropriate quality for (U-Th)/He analysis.

Last, the zircon (U-Th)/He age data presented here has little bearing on the age of deposition of the Pointe-a-Pierre Formation. As noted already, Vincent and Wach (2007) suggested a middle to late Eocene age based on fossil data, while Algar et al. (1998) suggested an Oligocene age based on detrital ZFT ages. The (U-Th)/He data presented here are consistent with both hypotheses and therefore provide no resolution to this debate.

CONCLUSIONS

AFT and (U-Th)/He zircon thermochronology provide new insights into the tectonic evolution of the Central Range of Trinidad (Fig. 6). The sandstones of the Chaudiere, Pointe-a-Pierre, and Nariva Formation have not experienced temperatures in excess of 180 °C during or after their burial in the Paleogene (Fig. 3). All three units preserve detrital (U-Th)/He zircon signals that most likely provide information about their South American provenance, i.e., the headwaters of a paleo–Oronoco River fan (?) system (Xie et al., 2010; Xie and Mann, 2014).

AFT age data consist of a heterogeneous population of single-grain ages with most samples failing the χ^2 test. Using D_{par} as a measure of resistance to annealing, 7 of 10 samples yielded a pooled AFT age of 15.6 ± 2.6 Ma. Minimum-age analysis (Galbraith, 2005; Vermeesch, 2009) suggested that the AFT data contain a younger cohort of grains with ages in the range of 13.3 ± 2.2 Ma (Fig. 5). These dates are statistically indistinguishable and, taken together, show that the Central Range experienced exhumation between 11 and 18 Ma.

The tectonic models of Speed (1985) and Pindell et al. (1998) have the Caribbean plate obliquely converging with the South American

TABLE 2. SUMMARY OF (U-Th)/He ZIRCON AGE DATA

Sample	w (μm)	l (μm)	Mass (μg)	U (ppm)	Th (ppm)	He (nmol/g)	eU (ppm)	Th/U	Raw date (Ma)	Ft*	Corr. date (Ma)	Analytical unc.* (1σ, Ma)
TT07-1b	124	207	14.8	163.2	104.6	430.7	187.7	0.6	406.7	0.854	**472.8**	8.5
TT07-1c	65	176	3.4	127.0	82.7	11.5	146.4	0.7	14.4	0.737	**19.6**	0.1
TT07-1z01	101	280	11.4	121.4	84.9	566.8	141.4	0.7	700.5	0.806	**869.2**	7.8
TT07-1z02	117	338	22.6	51.2	32.6	59.4	58.8	0.6	184.2	0.845	**218.1**	2.3
TT07-3a	73	209	5.1	73.4	63.4	433.9	88.3	0.9	830.7	0.766	**1049.9**	5.4
TT07-17a	65	175	3.4	558.3	153.3	99.9	594.3	0.3	30.9	0.732	**42.1**	0.6
TT07-17b	66	150	3.0	125.4	117.5	445.9	153.0	0.9	512.0	0.736	**682.5**	3.3
TT07-17c	63	138	2.5	154.2	48.2	35.6	165.5	0.3	39.5	0.719	**54.8**	0.3
TT07-18c	68	184	3.9	40.7	61.5	153.1	55.1	1.5	490.3	0.757	**638.2**	2.4
TT07-18b	61	176	3.1	87.3	69.2	378.1	103.6	0.8	632.0	0.729	**843.9**	3.6
TT08-1a	86	221	7.7	56.4	45.6	633.0	67.2	0.8	1423.4	0.797	**1646.5**	10.4
TT08-1b	58	230	3.6	341.0	273.7	52.3	405.3	0.8	23.7	0.722	**32.8**	0.3
TT08-1c	66	133	2.7	105.7	108.3	502.8	131.2	1.0	662.4	0.734	**878.5**	3.9
TT08-1z03	83	254	8.7	103.6	61.4	440.5	118.1	0.6	654.2	0.789	**828.9**	8.8
TT08-2a	62	183	3.2	89.3	139.8	411.0	122.2	1.6	588.5	0.736	**783.0**	3.4
TT08-2b	121	248	16.9	145.7	83.5	549.8	165.3	0.6	578.1	0.844	**676.8**	12.4
TT08-2c	76	183	4.9	103.1	79.7	491.5	121.9	0.8	692.8	0.769	**879.1**	5.1
TT08-3b	112	283	16.7	104.2	100.8	500.7	127.9	1.0	675.1	0.841	**791.4**	10.4
TT08-3c	74	202	5.1	319.1	282.0	482.3	385.4	0.9	226.0	0.767	**292.8**	3.3
TT08-4c	64	161	3.1	207.9	252.6	119.0	267.2	1.2	81.4	0.734	**110.7**	0.6
TT08-4a	64	142	2.7	329.0	317.7	352.1	403.6	1.0	158.5	0.728	**216.6**	1.5

Note: w—average width of zircons; l—length of zircons corrected for broken crystals; Mass—mass of the zircons; U—uranium concentration; Th—thorium concentration; He—helium concentration; eU—effective uranium; Ft*—α-ejection correction; Corr. date—date determined after correction for α-ejection; Analytical unc.*—analytical uncertainties propagated from U, Th, and He measurement uncertainties, excluding uncertainty on α-ejection.

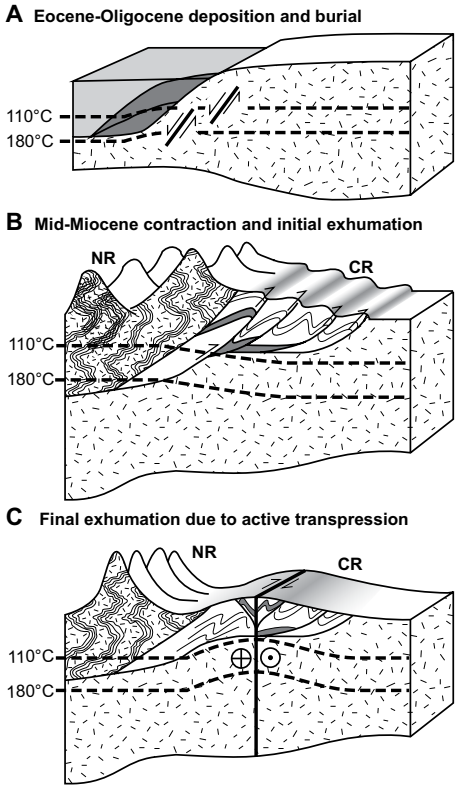

Figure 7. Tectonic model illustrating the deposition, burial, and exhumation history of the Central Range. The Eocene and Oligocene rocks units analyzed in this study are shown in dark gray. Each panel shows the current position of the apatite fission-track and (U-Th)/He isograds for that time step. (A) Following deposition, units were buried but did not reach depths sufficient to reset the (U-Th)/He zircon ages. (B) Contraction in the mid-Miocene resulted in exhumation through the 110 °C isograd, locking in the apatite fission-track ages. (C) Less than a few kilometers of exhumation due to possibly active transpression. Exhumation during this last event was not sufficient to bring rocks to the surface that have experienced temperatures in excess of 110 °C; therefore, the apatite fission-track thermochronology does not record this possible late stage of exhumation. NR—Northern Range; CR—Central Range.

plate in the middle Miocene. The presence of a middle Miocene angular unconformity is consistent with this interpretation (e.g., Kugler, 1960; Babb and Mann, 2000; Soto et al., 2011; Fig. 2A). The 18–11 Ma cooling event indicated by the AFT is consistent with exhumation driven by oblique convergence in the core of the Central Range uplift during this time period. Subsequent deformation due to modern transpression, if any is occurring, has not resulted in exhumation great enough to reset the AFT ages in the Central Range fault zone (i.e., <4 km of exhumation).

ACKNOWLEDGMENTS

Paul O'Sullivan, Raymond Donelick, and Margaret Donelick of Apatite to Zircon, Inc., performed the mineral separation and apatite fission-track analysis presented here. Benjamin Laabs and Dan Jacques assisted with the mineral separation for the (U-Th)/He analysis. John Tong, Jenna Hojnowski, Kathleen Sharman, William Pierce, and Mike Oliver provided field assistance. We thank Hasley Vincent, Chris Archie, Chris Lakhan, and John Dumas-Keens for access to sampling sites. Discussions with Annia Fayon, Pieter Vermeesch, Richard Ketcham, and Philip Farfan greatly improved this manuscript. This project was funded by donors to the Petroleum Research Foundation and the Geneseo Foundation.

REFERENCES CITED

Algar, S.T., Heady, E.C., and Pindell, J.L., 1998, Fission track dating in Trinidad: Implications for provenance, depositional timing, and tectonic uplift, *in* Pindell, J.L., and Drake, C.L, eds., Paleogeographic Evolution and Non-Glacial Eustasy, Northern South America: Society for Sedimentary Geology (SEPM) Special Publication 58, p. 111–128, doi:10.2110/pec.98.58.0111.

Babb, S., and Mann, P., 2000, Structural and sedimentary development of a Neogene transpressional plate boundary between the Caribbean and South American plates in Trinidad and the Gulf of Paria, *in* Mann, P., ed., Caribbean Basins: Amsterdam, Netherlands, Elsevier, p. 495–557.

Bolli, H.M., 1957, Planktonic foraminifera from the Eocene Navet and San Fernando formations of Trinidad, B.W.I., *in* Loeblich, A.R., Tappan, H., Beckmann, J.P., Bolli, H.M., Gallitelli, E.M., and Troelsen, J.C., eds., Studies in Foraminifera: Bulletin of the U.S. Natural History Museum 215, p. 155–172.

Carlson, W.D., Donelick, R.A., and Ketcham, R.A., 1999, Variability of apatite fission-track annealing kinetics: I. Experimental results: The American Mineralogist, v. 84, p. 1213–1223, doi:10.2138/am-1999-0901.

Christeson, G.L., Mann, P., Escalona, A., and Aitken, T.J., 2008, Crustal structure of the Caribbean–northeastern South America arc-continent collision zone: Journal of Geophysical Research, v. 113, doi:10.1029/2007JB005373.

Churches, C., Weber, J., Robertson, R., LaFemina, P., Geirsson, H., Shaw, K., Higgins, M., and Miller, K., 2014, New GPS evidence for continental transform fault creep, Central Range fault, Trinidad, and its geologic and hazard implications: Geological Society of America Abstracts with Programs, v. 46, no. 6, p. 360.

Cruz, L., Fayon, A., Teyssier, C., and Weber, J., 2007, Exhumation and deformation processes in transpressional orogens; the Venezuelan Paria Peninsula, SE Caribbean–South American plate boundary, *in* Till, A.B., Roeske, S.M., Sample, J.C., and Foster, D.A., eds., Exhumation Associated with Continental Strike-Slip Fault Systems: Geological Society of America Special Paper 434, p. 149–165, doi:10.1130/2007.2434(08).

de Verteuil, L., Ramlal, B., Weber, J., 2006, Trinidad Geological GIS, Module 1- Surface Geology and Geography: Port-of-Spain, Trinidad, Latinum, Ltd.

Denison, C., Weber, J., Donelick, R., and O'Sullivan, P., 2008, Apatite Fission-Track Thermochronology, Northern Range, Trinidad (and Paria Peninsula, Venezuela) [Ph.D. thesis]: Allendale, Michigan, Grand Valley State University, McNair Thesis Report, 39 p., http://scholarworks.gvsu.edu/cgi/viewcontent.cgi?article=1188&context=mcnair.

de Verteuil, L., Ramlal, B., and Weber, J., 2006, Trinidad Geological GIS, Module 1—Surface Geology and Geography: Port-of-Spain, Trinidad, Latinum, Ltd.

Donelick, R.A., 1993, A Method of Fission Track Analysis Utilizing Bulk Chemical Etching of Apatite: U.S. Patent 5267274.

Donelick, R.A., and Miller, D.S., 1991, Enhanced TINT fission track densities in low spontaneous track density apatites using ^{252}Cf-derived fission fragment tracks: A model and experimental observations: Nuclear Tracks and Radiation Measurements, v. 18, p. 301–307, doi:10.1016/1359-0189(91)90022-A.

Donelick, R.A., O'Sullivan, P.B., and Ketcham, R.A., 2005, Apatite fission-track analysis: Reviews in Mineralogy and Geochemistry, v. 58, p. 49–94, doi:10.2138/rmg.2005.58.3.

Erlich, R.N., Farfan, P.F., and Hallock, P., 1993, Biostratigraphy, depositional environments, and diagenesis of the Tamana Formation, Trinidad: A tectonic marker horizon: Sedimentology, v. 40, p. 743–768, doi:10.1111/j.1365-3091.1993.tb01358.x.

Flinch, J.F., Rambaran, V., Ali, W., de Lisa, V., Hernandez, G., Rodrigues, K., and Sams, R., 2000, Structure of the Gulf of Paria pull-apart basin (eastern Venezuela–Trinidad), *in* Mann, P., ed., Sedimentary Basins of the World: Volume 4. Caribbean Basins: Amsterdam, Elsevier, p. 477–494.

Galbraith, R.F., 2005, Statistics for Fission Track Analysis: Boca Raton, Chapman and Hall/CRC, Interdisciplinary Statistics Series, 224 p., doi:10.1201/9781420034929.

Giorgis, S., Tong, J., and Sirianni, R., 2009, Constraining neotectonic orogenesis using an isostatically compensated model of transpression: Journal of Structural Geology, v. 31, p. 1074–1083, doi:10.1016/j.jsg.2009.02.003.

Giorgis, S., Weber, J., Hojnowski, J., Pierce, W., and Rodriguez, A., 2011, Using orthographic projection with geographic information system (GIS) data to constrain the kinematics the Central Range fault zone, Trinidad: Journal of Structural Geology, v. 33, p. 1254–1264, doi:10.1016/j.jsg.2011.05.008.

Gleadow, A.J.W., Duddy, I.R., Green, F., and Lovering, J.F., 1986, Confined fission track lengths in apatite: A diagnostic tool for thermal history analysis: Contributions to Mineralogy and Petrology, v. 94, p. 405–415, doi:10.1007/BF00376334.

Green, P.F., Duddy, I.R., Gldeadow, A.J.W., and Lovering, J.F., 1989, Apatite fission track analysis as a paleotemperature indicator for hydrocarbon exploration, *in* Naeser, N.D., and McCullogh, T.H., eds., Thermal History of Sedimentary Basins: Methods and Case Histories: New York, Springer-Verlag, p. 181–195, doi:10.1007/978-1-4612-3492-0_11.

Guenthner, W.R., Reiners, P.W., Ketcham, R.A., Nasdala, L., and Giester, G., 2013, Helium diffusion in natural zircon: Radiation damage, anisotropy, and the interpretation of zircon (U-Th)/He thermochronology: American Journal of Science, v. 313, no. 3, p. 145–198, doi:10.2475/03.2013.01.

Ketcham, R.A., 2005, Forward and inverse modeling of low-temperature thermochronometry data: Reviews in Mineralogy and Geochemistry, v. 58, p. 275–314, doi:10.2138/rmg.2005.58.11.

Ketcham, R.A., Donelick, R.A., and Carlson, W.D., 1999, Variability of apatite fission-track annealing kinetics: III. Extrapolation to geological time scales: The American Mineralogist, v. 84, p. 1235–1255, doi:10.2138/am-1999-0903.

Ketcham, R.A., Donelick, R.A., and Donelick, M.B., 2000, AFTSolve: A program for multi- kinetic modeling of fission-track data: Geological Materials Research, v. 2, no. 1, p. 1–32.

Kugler, H., 1960, Geological Map of Trinidad with Cross-Sections: Basel, Switzerland, Orell Fussli Arts Graphiques S.A., scale 1:100,000.

Kugler, H.G., 2001, Treatise on the Geology of Trinidad: Part 4. Paleocene to Holocene formations, *in* Bolli, H.M., and Knappertsbusch, M., eds.: Basel, Switzerland, Museum of Natural History Basel, 309 p.

Parra, M., Mora, A., Lopez, C., Rojas, L.E., and Horton, B.K., 2012, Detecting earliest shortening and deformation advance in thrust belt hinterlands: Example from the Colombian Andes: Geology, v. 40, p. 175–178, doi:10.1130/G32519.1.

Pérez, O.J., Bilham, R., Bendick, R., Velandia, J.R., Hernández, N., Moncayo, C., Hoyer, M., and Kozuch, M.,

2001, Velocity field across the southern Caribbean plate boundary and estimates of Caribbean/South American plate motion using GPS geodesy 1994–2000: Geophysical Research Letters, v. 28, p. 2987–2990, doi:10.1029/2001GL013183.

Pindell, J.L., and Kennan, L., 2007, Cenozoic Kinematics and Dynamics of Oblique Collision Between two Convergent Plate Margins: The Caribbean-South America Collision in Eastern Venezuela, Trinidad and Barbados, Transactions of GCSSEPM 27th Annual Bob F. Perkins Research Conference, p. 458–553.

Pindell, J., Higgs, R., and Dewey, J., 1998, Cenozoic palinspastic reconstruction, paleogeographic evolution, and hydrocarbon setting of the northern margin of South America, *in* Pindell, J., and Drake, C., eds., Paleogeographic Evolution and Non-Glacial Eustasy, Northern South America: Society for Sedimentary Geology (SEPM) Special Publication 58, p. 45–85, doi:10.2110/pec.98.58.0045.

Prentice, C., Weber, J., Crosby, C., and Ragona, D., 2010, Prehistoric earthquakes on the Caribbean–South American plate boundary, Central Range fault, Trinidad: Geology, v. 38, no. 8, p. 675–678, doi:10.1130/G30927.1.

Russo, R.M., Okal, E.A., and Rowley, K.C., 1992, Historical seismicity of the southeastern Caribbean and tectonic implications: Pure and Applied Geophysics, v. 139, no. 1, p. 87–120, doi:10.1007/BF00876827.

Saleh, J., Edwards, K., Barbaste, J., Balkaransingh, S., Grant, D., Weber, J., and Leong, T., 2004, On some improvements in the geodetic framework of Trinidad and Tobago: Survey Review, v. 37, p. 604–625, doi:10.1179/sre.2004.37.294.604.

Saunders, J.B., 1998, Geological Map of Trinidad: Port of Spain, Trinidad, Ministry of Energy and Energy Industries, Government of the Republic of Trinidad and Tobago, scale: 1:100,000.

Soto, M.D., Mann, P., Escanola, A., and Wood, A.J., 2007, Late Holocene strike-slip offset of a subsurface channel interpreted from three-dimensional seismic data, eastern offshore Trinidad: Geology, v. 35, p. 859–862, doi:10.1130/G23738A.1.

Soto, D., Mann, P., and Escalona, A., 2011, Miocene-to-recent structure and basinal architecture along the Central Range strike-slip fault zone, eastern offshore Trinidad: Marine and Petroleum Geology, v. 28, p. 212–234.

Speed, R.C., 1985, Cenozoic collision of the Lesser Antilles arc and continental South America and the origin of the El Pilar fault: Tectonics, v. 4, p. 41–69, doi:10.1029/TC004i001p00041.

Tagami, T., and O'Sullivan, P.B., 2005, Fundamentals of fission-track thermochronology: Reviews in Mineralogy and Geochemistry, v. 58, p. 19–47, doi:10.2138/rmg.2005.58.2.

Teyssier, C., Tikoff, B., and Weber, J., 2002, Attachment between brittle and ductile crust at wrenching plate boundaries, *in* Bertotti, G., Schulmann, K., and Cloetingh, S.A.P.L., eds., Continental collision and the tectono-sedimentary evolution of forelands: European Geosciences Union Stephan Mueller Special Publication 1, p. 75–91, doi:10.5194/smsps-1-75-2002.

Vermeesch, P., 2009, RadialPlotter: A Java application for fission track, luminescence and other radial plots: Radiation Measurements, v. 44, p. 409–410, doi:10.1016/j.radmeas.2009.05.003.

Vincent, H., and Wach, G., 2007, Paleogene slope deposits; examples from the Chaudiere, Pointe-a-Pierre and San Fernando Formations, Central Range, Trinidad, *in* Kennan, L., Pindell, J., and Rosen, N.C., eds., The Paleogene of the Gulf of Mexico and Caribbean Basins: Processes, Events, and Petroleum Systems: Houston, Texas, Gulf Coast Section, Society for Sedimentary Geology (SEPM), p. 554–585.

Weber, J., Dixon, T.H., DeMets, C., Ambeh, W.B., Jansma, P., Mattioli, G., Saleh, J., Sella, G., Bilham, R., and Perez, O., 2001a, GPS estimate of relative motion between the Caribbean and South American plates, and geological implications for Trinidad and Venezuela: Geology, v. 29, p. 75–78, doi:10.1130/0091-7613(2001)029<0075:GEORMB>2.0.CO;2.

Weber, J., Ferrill, D., and Roden-Tice, M., 2001b, Calcite and quartz microstructural geothermometry of low-grade metasedimentary rocks, Northern Range, Trinidad: Journal of Structural Geology, v. 23, p. 93–112, doi:10.1016/S0191-8141(00)00066-3.

Weber, J., Saleh, J., Balkaransingh, S., Dixon, T., Ambeh, W., Leong, T., Rodriguez, A., and Miller, K., 2011, Triangulation-to-GPS and GPS-to-GPS geodesy in Trinidad, West Indies: Neotectonics, seismic risk, and geologic implications: Journal of Petroleum and Marine Geology, v. 28, p. 200–211, doi:10.1016/j.marpetgeo.2009.07.010.

Xie, X., and Mann, P., 2014, U-Pb detrital zircon age patterns of Cenozoic clastic sedimentary rocks in Trinidad and its implications: Sedimentary Geology, v. 307, p. 7–16, doi:10.1016/j.sedgeo.2014.04.001.

Xie, X., Mann, P., and Escalona, A., 2010, Regional provenance study of Eocene clastic sedimentary rocks within the South American–Caribbean plate boundary zone using detrital zircon geochronology: Earth and Planetary Science Letters, v. 291, p. 159–171, doi:10.1016/j.epsl.2010.01.009.

Science Editor: David I. Schofield
Associate Editor: Jon Pelletier

Manuscript Received 5 June 2015
Revised Manuscript Received 30 March 2016
Manuscript Accepted 6 July 2016

Printed in the USA